Influence of carnosine and carnosinase-1 on diabetes-induced afferent arteriole vasodilation

Rodriguez-Nino, Angelica; Pastene, Diego O.; Hettler, Steffen A.; Qiu, Jiedong; Albrecht, Thomas; Vajpayee, Srishti; Perciaccante, Rossana; Gretz, Norbert; Bakker, Stephan J. L.; Kraemer, Bernhard K.

Published in:
American journal of physiology-Renal physiology

DOI:
10.1152/ajprenal.00232.2021

Publication date:
2022

AMERICAN JOURNAL OF PHYSIOLOGY
RENAL PHYSIOLOGY

Am J Physiol Renal Physiol 323: F69–F80, 2022.
First published May 30, 2022; doi:10.1152/ajprenal.00232.2021

RESEARCH ARTICLE

Influence of carnosine and carnosinase-1 on diabetes-induced afferent arteriole vasodilation: implications for glomerular hemodynamics

Angelica Rodriguez-Niño,[1,2]* Diego O. Pastene,[2]* Steffen A. Hettler,[2] Jiedong Qiu,[2] Thomas Albrecht,[2] Srishti Vajpayee,[3] Rossana Perciaccante,[3] Norbert Gretz,[4] Stephan J. L. Bakker,[1] Bernhard K. Krämer,[2,5] Benito A. Yard,[2,5] and Jacob van den Born[1]

[1]*Department of Nephrology, University Medical Centre Groningen and University of Groningen, Groningen, The Netherlands;* [2]*Vth Medical Department, University Hospital Mannheim, Heidelberg University, Mannheim, Germany;* [3]*Cyanagen Srl, Bologna, Italy;* [4]*Central Medical Research Facility ZMF, University Hospital Mannheim, Heidelberg University, Mannheim, Germany; and* [5]*European Center for Angioscience, Mannheim, Germany*

Abstract

Dysregulation in glomerular hemodynamics favors hyperfiltration in diabetic kidney disease (DKD). Although carnosine supplementation ameliorates features of DKD, its effect on glomerular vasoregulation is not known. We assessed the influence of carnosine and carnosinase-1 (CN1) on afferent glomerular arteriole vasodilation and its association with glomerular size, hypertrophy, and nephrin expression in diabetic BTBR$^{ob/ob}$ mice. Two cohorts of mice including appropriate controls were studied: i.e., diabetic mice that received oral carnosine supplementation (*cohort 1*) and human (h)CN1 transgenic (TG) diabetic mice (*cohort 2*). The lumen area ratio (LAR) of the afferent arterioles and glomerular parameters were measured by conventional histology. Three-dimensional analysis using a tissue clearing strategy was also used. In both cohorts, LAR was significantly larger in diabetic BTBR$^{ob/ob}$ versus nondiabetic BTBR$^{wt/ob}$ mice (0.41 ± 0.05 vs. 0.26 ± 0.07, $P < 0.0001$ and 0.42 ± 0.06 vs. 0.29 ± 0.04, $P < 0.0001$) and associated with glomerular size (*cohort 1*: $r = 0.55$, $P = 0.001$ and *cohort 2*: $r = 0.89$, $P < 0.0001$). LAR was partially normalized by oral carnosine supplementation (0.34 ± 0.05 vs. 0.41 ± 0.05, $P = 0.004$) but did not differ between hCN1 TG and wild-type BTBR$^{ob/ob}$ mice. In hCN1 TG mice, serum CN1 concentrations correlated with LAR ($r = 0.90$, $P = 0.006$). Diabetic mice displayed decreased nephrin expression and increased glomerular hypertrophy. This was not significantly different in hCN1 TG BTBR$^{ob/ob}$ mice ($P = 0.06$ and $P = 0.08$, respectively). In conclusion, carnosine and CN1 may affect intraglomerular pressure in an opposing manner through the regulation of afferent arteriolar tone. This study corroborates previous findings on the role of carnosine in the progression of DKD.

NEW & NOTEWORTHY Dysregulation in glomerular hemodynamics favors hyperfiltration in diabetic kidney disease (DKD). Although carnosine supplementation ameliorates features of DKD, its effect on glomerular vasoregulation is not known. We assessed the influence of carnosine and carnosinase-1 (CN1) on afferent glomerular arteriole vasodilation and its association with glomerular size, hypertrophy, and nephrin expression in diabetic BTBR$^{ob/ob}$ mice. Our results provide evidence that carnosine feeding and CN1 overexpression likely affect intraglomerular pressure through vasoregulation of the afferent arteriole.

carnosine; carnosinase-1; diabetic kidney disease; glomerular hemodynamics; glomerular hyperfiltration

INTRODUCTION

Due to the increasing prevalence of diabetes (1), diabetic kidney disease (DKD) is the most common etiology of chronic kidney disease and end-stage renal disease in the Western world (2).

Glomerular hyperfiltration, defined as a supraphysiological increase in the glomerular filtration rate (GFR), is considered one of the primary events in the course of DKD. It has been proposed that this maladaptive response, comprising tubular and vascular factors, causes vasodilation and vasoconstriction of the afferent and efferent arterioles, respectively, thereby increasing intraglomerular pressure (3, 4). Obesity (5), hyperglycemia (6), and unbalanced insulin levels (7) play important roles in glomerular hemodynamic dysregulation. It is believed that in diabetes glomerular hemodynamic dysregulation precedes the onset and/or progression of albuminuria (8, 9) and overall predisposes to nephron damage by increasing intraglomerular hydraulic pressure (3). These changes in glomerular hemodynamics are often accompanied by morphological and ultrastructural events characterized by kidney size enlargement, an increase in the filtration surface area of the glomerulus (3), and glomerular and tubular hypertrophy (10).

A number of studies have shown that carnosine (β-alanyl-L-histidine), a naturally occurring dipeptide with antiglycating and antioxidating properties (11, 12), improves metabolic

*A. Rodriguez-Niño and D. O. Pastene contributed equally to this work.
Correspondence: D. O. Pastene (diego.pastene@medma.uni-heidelberg.de).
Submitted 15 June 2021 / Revised 12 May 2022 / Accepted 12 May 2022

profiles of diabetes and affords protection against DKD progression. As such, carnosine supplementation improves hyperglycemia and enhances insulin secretion in mouse models of type 2 diabetes (13, 14). In Zucker obese and streptozotocin-induced diabetic rats, carnosine ameliorates dyslipidemia (15, 16), attenuates albuminuria, restores glomerular ultrastructure, and prevents podocyte loss (17).

A potential protective role for carnosine in DKD has also been disclosed in genetic studies in humans, which identified the gene for the carnosine hydrolyzing enzyme carnosinase-1 (CN1), i.e., carnosinase dipeptidase 1 (*CNDP1*), as a risk factor for developing DKD (18–22). A 3-nt (CTG) repeat polymorphism in the signal peptide sequence of the *CNDP1* gene influences CN1 secretion (23) and correlates with serum CN1 concentrations. Based on the current evidence, it has been put forward that patients carrying the short $(CTG)_5$ *CNDP1* allelic variant have a lower risk to develop DKD because of low serum CN1 concentrations, which, in principle, allow higher tissue carnosine levels (23).

In line with this, overexpression of human (h)CN1 in mice reduces tissue carnosine levels, aggravates albuminuria, and worsens glomerular structural changes observed under diabetic conditions (14, 24, 25).

The profound effects of carnosine feeding and hCN1 overexpression on metabolic and renal histopathological parameters in the kidney (13, 14, 24, 25) are suggestive of changes in glomerular hyperfiltration and thereby in intraglomerular pressure.

Thus, the aim of this study was to investigate whether carnosine supplementation and overexpression of hCN1 affect glomerular hemodynamics through changes in the afferent arteriolar tone of diabetic mice. To this end, we used the BTBR$^{ob/ob}$ mouse model (26), which develops obesity, hyperglycemia, and hyperfiltration (27) and recapitulates many of the typical characteristics of human DKD in the late stages of the disease (26). We made use of conventional histology and a tissue clearing and perfusion staining methodology for three-dimensional (3D) analysis to estimate glomerular size and dilation of the afferent arteriole as indirect estimations of increased intraglomerular pressure.

MATERIALS AND METHODS

The experimental protocols and all animal procedures were approved by the "Regierungspräsidum Karlsruhe" (AZ 35-9185.81/G-119/11, AZ 35-9185.81/G-108/13, AZ 35-9185.81/G-116/14, AZ 35-9185.81/G-135/18, and AZ 35-9185.81/G-199/19) and were performed in accordance with the Principles of Laboratory Animal Care.

Experimental Design

Mice were housed in a specific pathogen-free and regularly monitored animal facility of the University of Heidelberg at 22°C at a 12:12-h light-dark cycle. They were fed regular chow and water ad libitum.

Carnosine levels were manipulated in BTBR$^{ob/ob}$ diabetic mice by two experimental approaches and compared with control BTBR$^{ob/ob}$ and healthy (wild-type, BTBR$^{wt/ob}$) mice, which are not leptin-deficient. Mice were either subjected to carnosine supplementation or genetically manipulated by overexpressing hCN1. These interventions were tested in separated experimental groups allowing appropriate control groups and comparisons. Clinical and laboratory parameters from these mice have been previously reported in studies by Albrecht et al. (13) and Qiu et al. (25).

Carnosine supplementation study.

Six-week-old male mice were purchased from Jackson Laboratories and divided into the following three groups: BTBR$^{wt/ob}$ mice (n = 5), BTBR$^{ob/ob}$ mice (n = 12), and BTBR$^{ob/ob}$ mice fed with carnosine (n = 14) dissolved in drinking water (45 mg/kg body wt), as previously reported (3). The stability of carnosine in the drinking water was ensured by replacing the drinking bottles every third day. After 18 wk of treatment (24 wk of age), blood samples were collected from the orbital plexus under isoflurane anesthesia.

hCN1 overexpression study.

hCN1 transgenic (TG) female and male mice were generated in the BTBR$^{wt/ob}$ strain as previously described in a study by Sauerhöfer et al. (14). Six-week-old BTBR$^{wt/ob}$ (2 females and 4 males, total n = 6), BTBR$^{ob/ob}$ (7 females and 3 males, total n = 10), and hCN1 TG BTBR$^{ob/ob}$ (4 females and 3 males, total n = 7) mice were included in these experiments.

All mice from both cohorts were euthanized at *week 24* of age by means of vascular perfusion through the aorta with 4% paraformaldehyde under ketamine and xylazine anesthesia.

Renal function study.

Eight-week-old male BTBR$^{ob/ob}$ mice were treated for 16 wk with carnosine via drinking water (n = 8) or fed with mouse chow containing a Na^+-glucose transporter-2 (SGLT2) inhibitor (60 mg/kg empagliflozin, kindly supplied by Boehringer Ingelheim), resulting in an average daily intake of 17.4 ± 4.3 mg/kg body wt (n = 6). Male wild-type mice (n = 4) and untreated diabetic mice (n = 7) of 24 wk of age were also included. FITC-sinistrin clearance was evaluated as previously described by Schreiber et al. (28). In brief, a bolus of FITC-sinistrin (Fresenius–Kabi) is injected via a tail vein while a transcutaneous device (MediBeacon) is placed on the naked skin of the mouse. The half-life time clearance of the compound registered by the device was used to determine GFR according to the empirical equation reported in Ref. 28. GFR measurements were conducted at 24 wk of age.

Serum CN1 Concentrations

CN1 concentrations in serum were assessed by ELISA in BTBR$^{ob/ob}$ hCN1 mice by an in-house developed ELISA system, as previously described (29).

Histological Analyses

After 4% paraformaldehyde perfusion, the kidneys were isolated, weighed, and embedded in paraffin. Three-micrometer sections were cut, deparaffinized with xylol, and rehydrated using an ethanol gradient. Sections were double immunostained with renin and α-smooth muscle actin, allowing identification of the afferent arterioles. The inner (lumen) and outer vessel areas (μm^2) of randomly chosen afferent arterioles were measured with ImageJ software. The corrected lumen area was calculated as the inner lumen area (μm^2)-to-

outer vessel area (μm^2) ratio. This approach allowed us to standardize the measurements of all the analyzed afferent vessels in different planes, i.e., transversal, and longitudinal. Surface areas (μm^2) of 15–20 glomeruli per animal were randomly chosen and measured with ImageJ software to examine glomerular hypertrophy.

Tissue Clearing and 3D Analysis

A 3D semiautomated morphometrical analysis was conducted in 24-wk-old $BTBR^{wt/ob}$ (n = 4) and $BTBR^{ob/ob}$ (n = 4) mice with a solvent-based tissue clearing and perfusion staining methodology as previously described (30) in 1- to 2-mm kidney portions. The dye used for vascular staining was SV620C-01-PEI, which has been designed based on three characteristics essential for renal vascular staining: cationic charge to ensure electrostatic interactions with the negatively charged endothelium, a molecular weight of more than 50 kDa to prevent filtration by the glomeruli, and a hydrodynamic diameter of more than 6 nm to prevent leakage through the vascular fenestrations. These properties combined gave SV620C-01-PEI an overall cationic charge and molecular weight of roughly 70 kDa, with an absorption maxima at 620 nm and emission in the infrared region with the emission maxima at 750 nm.

Maximum glomerular diameter (Feret's size) and a cross-sectional diameter of the afferent arteriole were measured in 30 glomeruli per mice in random 1-mm^3 optical sections. Afferent arterioles were identified by inspection of vascular branches and defined as the arteriole connecting a single glomerular tuft with a main vessel without ramification. Image acquisition was performed with a double light-sheet microscope (DLS TCS SP8, Leica Microsystems) using Leica Application Suite X software (LASX v.3.5.6, Leica Microsystems). Presegmentation, processing, and measuring were performed using FIJI (ImageJ 1.52p) with the ImageJ apps: 3D Objects Counter (31) and 3 D ImageJ Suite (3DSuite) (32) on segmented files for Feret's size quantification. Segmentation was performed using Ilastik (v.1.3.2).

Immunofluorescence

Double immunostaining of α-smooth muscle actin and renin, antigen retrieval was performed using Tris·HCl buffer (0.1 M, pH 9.0) at 85°C overnight. Endogenous peroxidase activity was blocked with 0.3% hydrogen peroxide. Sections were incubated with mouse anti-human smooth muscle actin (1:500, Dako, Glostrup, Denmark) followed by goat anti-mouse IgG2a horseradish peroxidase-labeled secondary antibody (1:50, SouthernBiotech) and donkey anti-goat IgG horseradish peroxidase-labeled tertiary antibody (1:50, SouthernBiotech). Horseradish peroxidase activity was visualized using the tetramethylrhodamine system (Perkin-Elmer LAS). Thereafter, for renin staining, sections were incubated overnight at 4°C with rabbit anti-mouse renin (1:2,000) kindly provided by Dr. T. Inagami (Vanderbilt University School of Medicine, Nashville, TN) (33), followed by secondary goat anti-rabbit FITC-conjugated antibody (1:100, SouthernBiotech). After extensive washing, DAPI solution was added to the sections for nuclear staining. As negative controls, the primary antibodies were replaced by PBS to control the cross-binding of the conjugates. To reduce autofluorescence, sections were incubated with Sudan black (0.15% in 70% ethanol) for 5 min and thereafter washed extensively. Immunofluorescence was visualized using a Leica DM4000B microscope equipped with a DFX345FX camera using the LASv4 software package. Eight pictures at ×200 magnification per kidney were taken with identical exposure settings and thereafter quantified with ImageJ software with standardized threshold settings.

Nephrin staining was performed after antigen retrieval by 10 mM TRIS-1 mM EDTA buffer (pH 9.0) for 30 min in a microwave. Endogenous peroxidase activity was blocked with 0.3% hydrogen peroxide. Unspecific binding was reduced by incubation with 5% rabbit serum. Sections were incubated overnight with goat anti-mouse nephrin antibody (1:100, R&D) diluted in 1% rabbit serum and 0.1% Triton X-100. After extensive washing, sections were incubated with rabbit anti-goat horseradish peroxidase-labeled secondary antibody (1:100, Dako) diluted in 1% rabbit serum and 0.1% Triton X-100. Horseradish peroxidase activity was visualized using the tetramethylrhodamine system (Perkin-Elmer LAS). DAPI solution was added to counterstain the nuclei. Eight pictures at ×100 magnification were taken per kidney with identical exposure settings and thereafter quantified by ImageJ software with standardized threshold settings and expressed as the positively stained percent area per glomerulus.

Statistical Analysis

Data are expressed as means ± SD. We performed a one-way ANOVA test followed by a Tukey's post hoc test to assess the effect of the interventions, e.g., carnosine supplementation and overexpression of hCN1 on the afferent arteriole corrected lumen area, glomerular size, and nephrin expression. To compare two groups, unpaired two-sided t tests were performed. Correlations were assessed by means of a two-sided Pearson correlation test. Due to a skewed distribution, the albumin-to-creatinine ratio (ACR) was 2-base logarithmically transformed ($\log_2$) and used as such in the correlation analyses. In addition, data on the afferent lumen area ratio (LAR), glomerular size, and nephrin expression from carnosine-fed and hCN1 TG mice were normalized by the geometric mean value of their respective untreated diabetic control group and expressed as a percent, allowing for comparison of the two cohorts. A two-sided P value of <0.05 was considered as statistically significant. GraphPad Prism 8.0 and JMP software were used for analyses and creation of the figures.

RESULTS

First, we made use of a combination of perfusion staining, ethyl-cinnamate clearing, and 3D imaging of kidney tissue from BTBR mice. This protocol, as previously described in the literature (30), allowed us to clearly visualize the renal vascular network, i.e., high-order branches of blood vessels, the afferent and efferent arterioles, and the glomerular tuft, which are displayed as bright fluorescent signals in a 3D stack (Fig. 1A). By virtue of a high signal-to-noise ratio due to optical sectioning, this approach facilitates the independent segmentation of glomerular tufts for their morphometrical

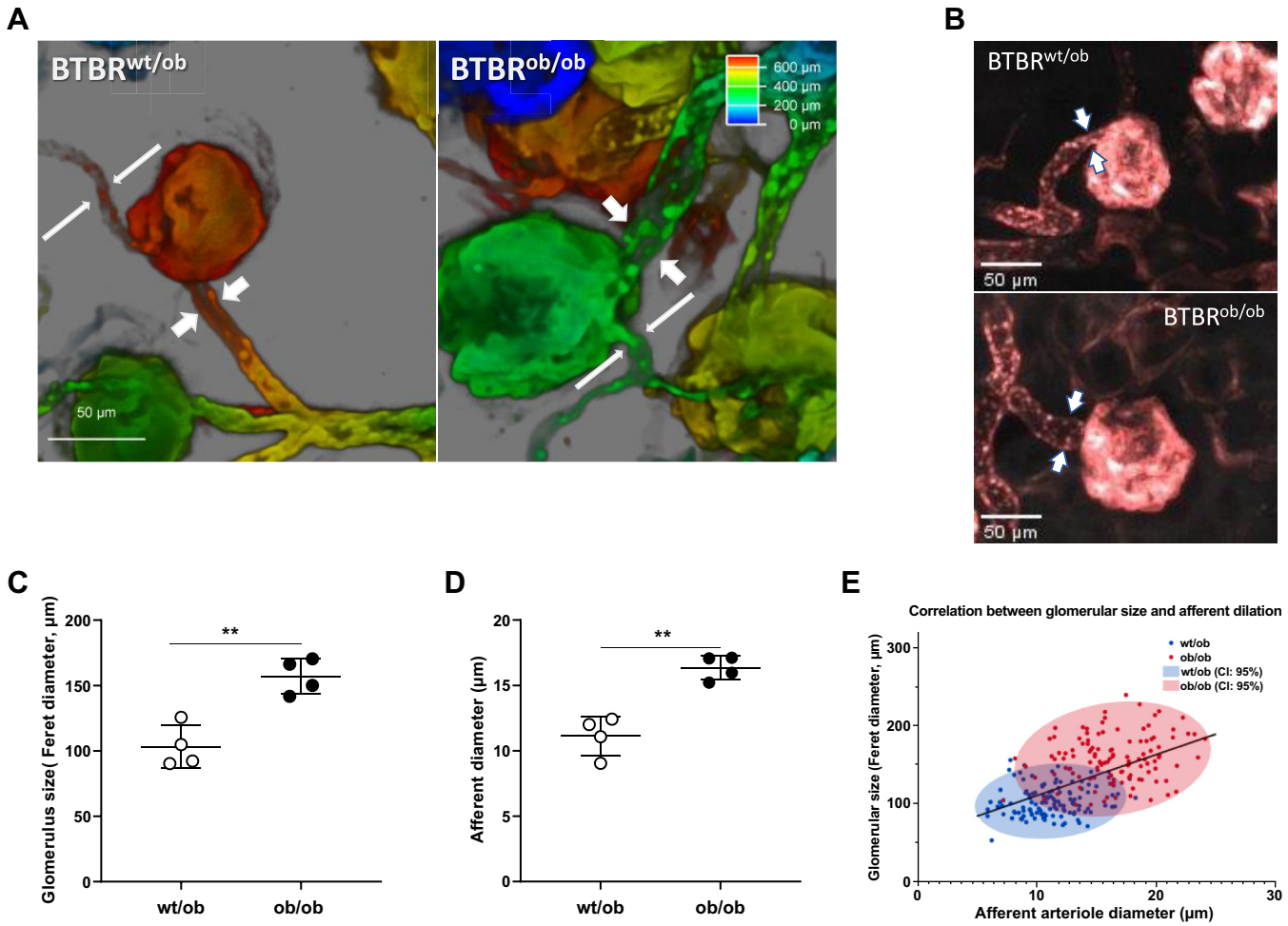

Figure 1. Three-dimensional analysis of glomerulus and renal microvasculature in the BTBR mouse model. *A*: three-dimensional reconstruction of a vascular branch with glomeruli whose afferent (short arrow) and efferent (long arrow) arterioles were imaged in a BTBR$^{wt/ob}$ mouse (*left*) and BTBR$^{ob/ob}$ mouse (*right*) using a light-sheet microscope after perfusion with a cationic red/infrared fluorophore and clearing with ethyl cinnamate. The bar represents depth with color coding. *B*: representative orthogonal projections of BTBR$^{wt/ob}$ and BTBR$^{ob/ob}$ phenotypes, where the afferent arteriolar diameter was measured (between the white arrows). *C* and *D*: three-dimensional diameter (Feret, µm) of 30 glomeruli (*C*) and cross-sectional diameter (µm; *D*) of afferent arterioles of BTBR$^{wt/ob}$ (n = 4) and BTBR$^{ob/ob}$ (n = 4) mice. Data are depicted as means ± SD. $^{**}P < 0.001$. An unpaired two-sided t test was used to compare groups. *E*: bivariate correlation between afferent arteriole diameter and glomerular size measured by the three-dimensional approach. Each dot represents the paired observation of afferent arteriole estimated diameter (x-axis) and Feret's diameter of the correspondent tuft (y-axis) of a glomerulus. Between 27 and 30 glomeruli were measured per mouse. An overall positive linear correlation was observed between the two variables (black line, r = 0.56, $P > 0.0001$). Shadowed areas represent the 95% confidence interval (CI) of BTBR$^{wt/ob}$ mice (blue, n = 4) and diabetic mice (red, n = 4). Correlations were assessed with a two-sided Pearson correlation test.

analysis and the estimation of the diameter of their corresponding afferent arterioles (Fig. 1*B*).

In kidneys analyzed by this method, maximum glomerular diameter (Feret's diameter) was significantly increased in diabetic versus nondiabetic mice (157.2 ± 13.5 vs. 103.3 ± 16.3 µm, P = 0.002; Fig. 1*C*). Furthermore, the estimated diameter of afferent arterioles in BTBR$^{ob/ob}$ mice was found to be enlarged compared with BTBR$^{wt/ob}$ mice (16.3 ± 0.92 vs. 11.1 ± 1.5 µm, P = 0.001; Fig. 1*D*). The diameter of efferent arterioles could not be accurately estimated due to a low signal-to-noise ratio. Nevertheless, efferent arterioles of BTBR$^{ob/ob}$ and wild-type mice had a comparable vascular diameter under visual inspection (Fig. 1*A*). A positive correlation was observed between the estimated afferent diameter and the Feret's diameter of the corresponding glomerular tuft derived from the 3D analysis (n = 237 glomeruli, r = 0.56, $P < 0.0001$; Fig. 1*E*).

Having observed changes compatible with increased intraglomerular pressure and hemodynamic dysregulation in BTBR$^{ob/ob}$ versus BTBR$^{wt/ob}$ mice, we assessed the influence of the carnosine/CN1 system on glomerular hemodynamics in diabetic mice. We made use of renal specimens that were collected in our previous studies (13, 25). However, because perfusion staining was not performed, a different approach, i.e., conventional histology, was used to address this question. Two different interventions were tested, i.e., carnosine supplementation and overexpression of hCN1 in BTBR$^{ob/ob}$ mice.

Untreated BTBR$^{ob/ob}$ mice developed increased body weight as well as albuminuria and increased HbA1c compared with BTBR$^{wt/ob}$ mice. Carnosine supplementation in BTBR$^{ob/ob}$ mice did not influence body weight but reduced albuminuria and HbA1c significantly. Compared with diabetic mice, hCN1 TG BTBR$^{ob/ob}$ mice displayed significantly lower body weight and developed higher albuminuria and HbA1c levels with

borderline significance (Supplemental Table S1, https://doi.org/10.6084/m9.figshare.14779971). Renal and metabolic parameters from these animals have been previously described in detail in studies by Albrecht et al. (13) and Qiu et al. (25). We also assessed the effect of sex on diabetes and DKD-associated parameters. Kidney weight was significantly higher in BTBR$^{wt/ob}$ males versus BTBR$^{wt/ob}$ females. This was also the case for the comparison between male BTBR$^{ob/ob}$ and female BTBR$^{ob/ob}$ mice. HbA1c was higher in females than in males from the BTBR$^{ob/ob}$ group (Table 1).

We determined LAR of the afferent arteriole and compared it with untreated diabetic BTBR$^{ob/ob}$ and nondiabetic BTBR$^{wt/ob}$ mice. LAR of afferent arterioles in diabetic BTBR$^{ob/ob}$ mice was significantly larger compared with nondiabetic BTBR$^{wt/ob}$ mice (0.41 ± 0.05 vs. 0.26 ± 0.07, $P < 0.0001$; Fig. 2*A*). Partial normalization of the afferent LAR was observed in BTBR$^{ob/ob}$ mice that were orally supplemented with carnosine for 18 wk (0.34 ± 0.05 vs. 0.41 ± 0.05, $P = 0.004$, treated vs. untreated BTBR$^{ob/ob}$ mice; Fig. 2*A*).

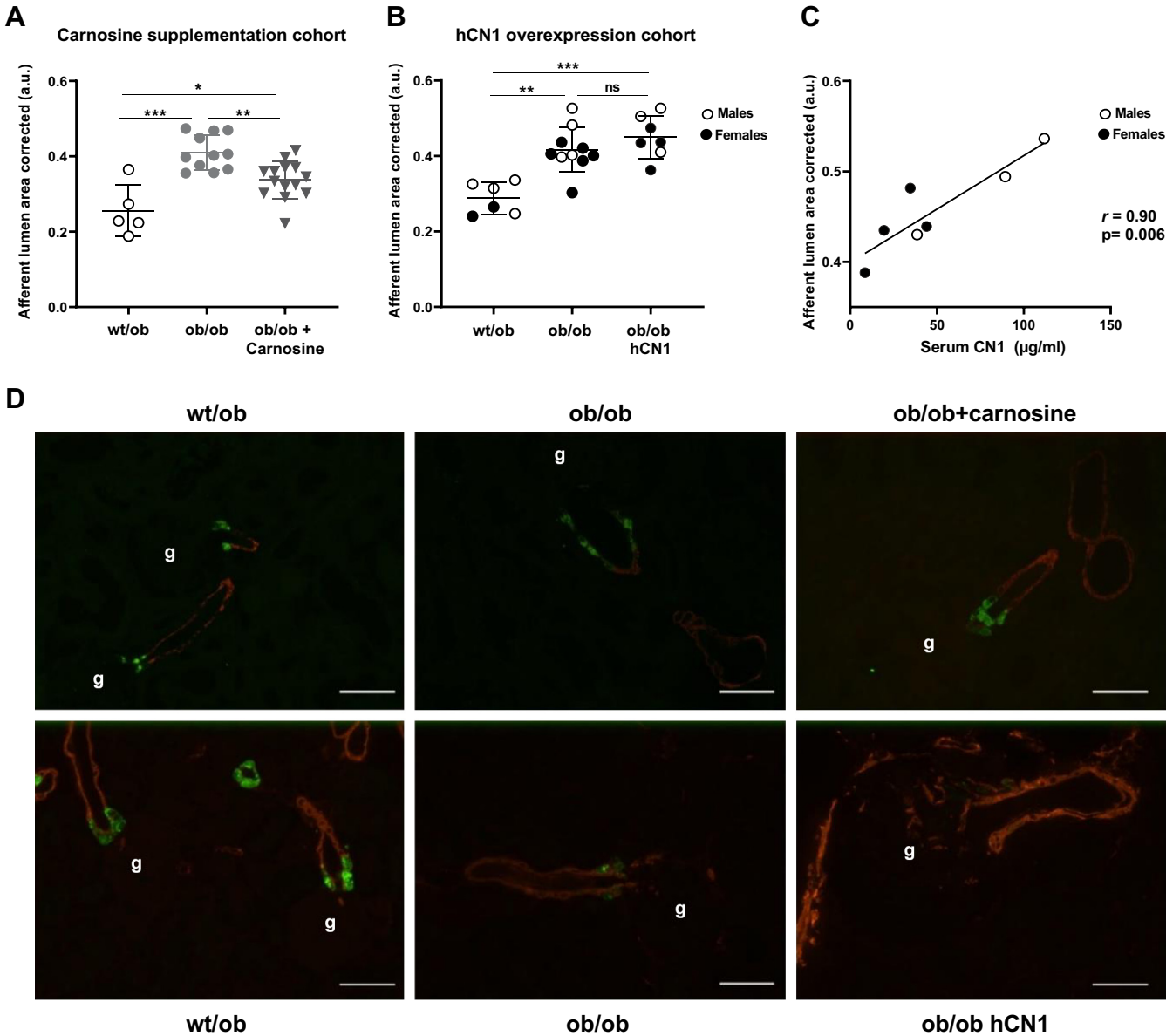

Figure 2. Opposite effects of carnosine supplementation and human (h) carnosinase-1 (CN1) overexpression on the afferent arteriole lumen in BTBR$^{ob/ob}$ mice. *A*: the afferent arteriole lumen was significantly enlarged in BTBR$^{ob/ob}$ mice compared with BTBR$^{wt/ob}$ mice. Carnosine supplementation for 18 wk in BTBR$^{ob/ob}$ mice partially normalized the enlargement of the afferent arteriole lumen. *B*: in a separate experiment, the lumen of afferent arterioles of BTBR$^{ob/ob}$ mice was also enlarged. *C*: although the afferent arteriole lumen area in BTBR$^{ob/ob}$ mice overexpressing hCN1 did not significantly differ from nontransgenic BTBR$^{ob/ob}$ mice, the concentrations of serum CN1 in BTBR$^{ob/ob}$ hCN1 mice strongly correlated with the degree of enlargement of the afferent arteriole lumen. *D*: representative images of afferent arterioles identified by double immunofluorescent staining of renin (green) and α-smooth muscle actin (orange) in kidneys sections of 24-wk-old BTBR$^{wt/ob}$ mice, BTBR$^{ob/ob}$ mice, BTBR$^{ob/ob}$ mice fed with carnosine, and BTBR$^{ob/ob}$ hCN1 transgenic mice. Scale bars = 50 µm. Data are depicted as means ± SD. *$P < 0.05$, **$P < 0.01$, and ***$P < 0.0001$. ns, $P > 0.05$. One-way ANOVA followed by a Tukey's post hoc test was used to compare groups. Correlation was assessed with a two-sided Pearson correlation test. a.u., arbitrary units; g, glomerulus.

In a second independent cohort consisting of nondiabetic BTBR$^{wt/ob}$, BTBR$^{ob/ob}$, and hCN1 TG BTBR$^{ob/ob}$ mice, a similar difference in LAR of the afferent arteriole was observed between BTBR$^{ob/ob}$ and nondiabetic mice (0.42 ± 0.06 vs. 0.29 ± 0.04, $P < 0.0001$) as in the first cohort (Fig. 2*B*).

When LAR in both cohorts was normalized for the corresponding diabetic control groups, the percentage of LAR change relative to the diabetic control in hCN1 BTBR$^{ob/ob}$ mice was significantly larger compared with carnosine-supplemented mice (8% vs. −17%, $P = 0.0001$; Supplemental Fig. S1*A*).

Since the vascular tone of the efferent arteriole also contributes to intraglomerular pressure, we measured the LAR of the efferent vessel. No differences were found among BTBR$^{wt/ob}$, untreated BTBR$^{ob/ob}$, and carnosine-fed BTBR$^{ob/ob}$ mice (data not shown).

Because serum CN1 concentrations in the hCN1 TG BTBR$^{ob/ob}$ group largely varied between individual mice, ranging from 8.6 to 111.8 μg/mL, we tested for a possible association between serum CN1 concentration and LAR. Serum CN1 concentrations were strongly and positively associated with LAR of the afferent arteriole (r =0.90, $P = 0.006$; Fig. 2*C*). As expected, CN1 was only expressed in TG mice and was undetectable in the serum of nondiabetic or non-TG BTBR$^{ob/ob}$ mice (data not shown). Interestingly, among hCN1 TG BTBR$^{ob/ob}$ mice, males appeared to have approximately threefold higher serum CN1 concentrations compared with hCN1 BTBR$^{ob/ob}$ females (26.7 ± 15.7 vs. 80 ± 37.5 μg/mL, $P <$ 0.05; Table 1).

Representative images of afferent arterioles, identified by double staining for renin and α-smooth muscle actin, from nondiabetic BTBR$^{wt/ob}$ mice, untreated BTBR$^{ob/ob}$ mice, and BTBR$^{ob/ob}$ mice orally supplemented with carnosine or overexpressing hCN1 are shown in Fig. 2*D*. Of note, we observed that afferent arterioles in some hCN1 TG BTBR$^{ob/ob}$ mice were notoriously larger (Fig. 2*D*, *bottom right*), particularly in those that displayed high serum CN1 concentrations (Fig. 2*C*).

As an indirect consequence of glomerular hemodynamic dysregulation in diabetes, we examined glomerular hypertrophy by measuring the total glomerular area. The glomerular area was almost doubled in *BTBR*$^{ob/ob}$ mice compared with BTBR$^{wt/ob}$ mice in both experiments (*cohort 1*: 8,310 ± 1,331 vs. 4,496 ± 839 μm^2, $P < 0.0001$, and *cohort 2*: 6,979 ± 894 vs. 4,219 ± 328 μm^2, $P < 0.0001$; Fig. 3). Although the total glomerular area tended to be lower in the carnosine supplementation group (8,310 ± 1,331 vs. 7,431 ± 1,201 μm^2, $P =$ 0.17; Fig. 3*A*), there was a tendency for further glomerular enlargement in the hCN1 TG group (7,837 ± 845 vs. 6,979 ± 894 μm^2, $P = 0.08$; Fig. 3*B*). Similar as shown for LAR, normalization of the glomerular area in both experiments revealed a significant increase in the hCN1 TG group versus the carnosine supplementation group (12% vs. −11%, $P <$ 0.05; Supplemental Fig. S1*B*). Furthermore, the glomerular area was positively associated with LAR of the afferent arteriole in the two different cohorts: carnosine supplementation ($n = 30$, $r = 0.55$, $P = 0.001$) and overexpression of hCN1 ($n =$ 23, $r = 0.89$, $P < 0.0001$; Fig. 3, *C* and *D*).

Next, we examined the expression of the slit diaphragm marker nephrin, which is essential for the maintenance of the glomerular filtration barrier and affected under high intraglomerular pressure conditions (34). Nephrin expression per glomerulus was significantly reduced in diabetic BTBR$^{ob/ob}$ versus nondiabetic BTBR$^{wt/ob}$ mice in both experiments (*cohort 1*: 40 ± 8% vs. 61 ± 4%, $P = 0.0003$, and *cohort 2*: 38 ± 9% vs. 67 ± 4%, $P < 0.0001$; Fig. 4).

Although carnosine supplementation did not significantly restore nephrin expression (47 ± 8% vs. 40 ± 8%, $P = 0.12$; Fig. 4*A*), nephrin expression was further reduced with borderline significance in hCN1 TG BTBR$^{ob/ob}$ mice (27 ± 12% vs. 38 ± 9%, $P = 0.06$; Fig. 4*B*). The percentage of nephrin expression relative to the untreated diabetic control group was significantly increased in the carnosine supplementation group versus the hCN1 group (16% vs. −28%, $P < 0.05$; Supplemental Fig. S1*C*). Representative images of nephrin immunostaining are shown in Fig. 4*C*.

In both cohorts, nephrin expression was inversely associated with the ACR (*cohort 1*: $n = 30$, $r = -0.59$, $P = 0.001$, and *cohort 2*: $n = 23$, $r = -0.78$, $P < 0.0001$; Fig. 5, *A* and *D*), with glomerular size (*cohort 1*: $r = -0.57$, $P = 0.001$, and *cohort 2*: $r = -0.75$, $P < 0.0001$; Fig. 5, *B* and *E*) and LAR (*cohort 1*: $r =$ −0.58, $P = 0.001$, and *cohort 2*: $r = -0.65$, $P = 0.0008$; Fig. 5, *C* and *F*). Interestingly, the afferent LAR was positively associated with HbA1c in both experimental groups (*cohort 1*: $n =$ 30, $r = 0.66$, $P = 0.001$, and *cohort 2*: $n = 23$, $r = 0.78$, $P <$ 0.0001; Supplemental Fig. S2).

A third cohort of BTBR mice was added to our study to assess renal functional changes associated with carnosine supplementation, in which BTBR$^{ob/ob}$ mice treated with a SGLT2 inhibitor were included to compare GFR normalization (Fig. 6). GFR of untreated BTBR$^{ob/ob}$ mice did not differ from SGLT2-treated mice (0.64 ± 0.11 vs. 0.64 ± 0.06 mL/min, $P >$ 0.9) or from carnosine-supplemented mice (0.67 ± 0.15 mL/

Table 1. *Sex comparison in cohort 2*

Parameter	BTBR$^{wt/ob}$			BTBR$^{ob/ob}$			hCN1 BTBR$^{ob/ob}$		
	Female	Male	*P* Value	Female	Male	*P* Value	Female	Male	*P* Value
Body weight, g	29.8 ± 5.0	35.2 ± 2.8	0.14	70.5 ± 1.3	70.4 ± 5.4	0.95	59.0 ± 5.9	65.3 ± 2.2	0.14
Kidney weight, g	0.22 ± 0.02	0.29 ± 0.01	0.006*	0.35 ± 0.03	0.48 ± 0.07	0.002*	0.36 ± 0.06	0.41 ± 0.02	0.26
HbA1c, %	4.7 ± 0.14	4.9 ± 0.19	0.39	7.7 ± 1.04	10.3 ± 0.46	0.004*	9.9 ± 0.46	9.4 ± 0.06	0.10
Albumin-to-creatinine ratio, μg/mL	92.1 ± 0.0	48.6 ± 12.4	0.05	561.5 ± 308.0	700.0 ± 368.1	0.55	1,290 ± 665.0	738.8 ± 257.9	0.27
Afferent lumen area ratio, arbitrary units	0.25 ± 0.02	0.31 ± 0.04	0.16	0.39 ± 0.04	0.47 ± 0.04	0.06	0.43 ± 0.04	0.48 ± 0.06	0.25
Glomerular area, μm^2	3,903 ± 323	4,377 ± 209	0.09	6,860 ± 964	7,256 ± 802	0.55	7,511 ± 907	8,272 ± 644	0.27
Nephrin expression, %	65.9 ± 2.2	68.0 ± 4.9	0.60	37.7 ± 10.4	38.4 ± 2.6	0.91	25.0 ± 10.9	30.6 ± 14.5	0.58
Serum CN1, μg/mL							26.7 ± 15.7	80 ± 37.5	0.04*

Data are presented as means ± SD. The effects of sex on diabetes and on diabetic nephropathy-associated parameters in BTBR$^{wt/ob}$, BTBR$^{ob/ob}$, and human (h) carnosinase-1 (CN1) BTBR$^{ob/ob}$ mice from *cohort 2* at 24 wk of age were assessed by an independent *t* test. *Significantly different ($P < 0.05$) from the opposite sex in the same group.

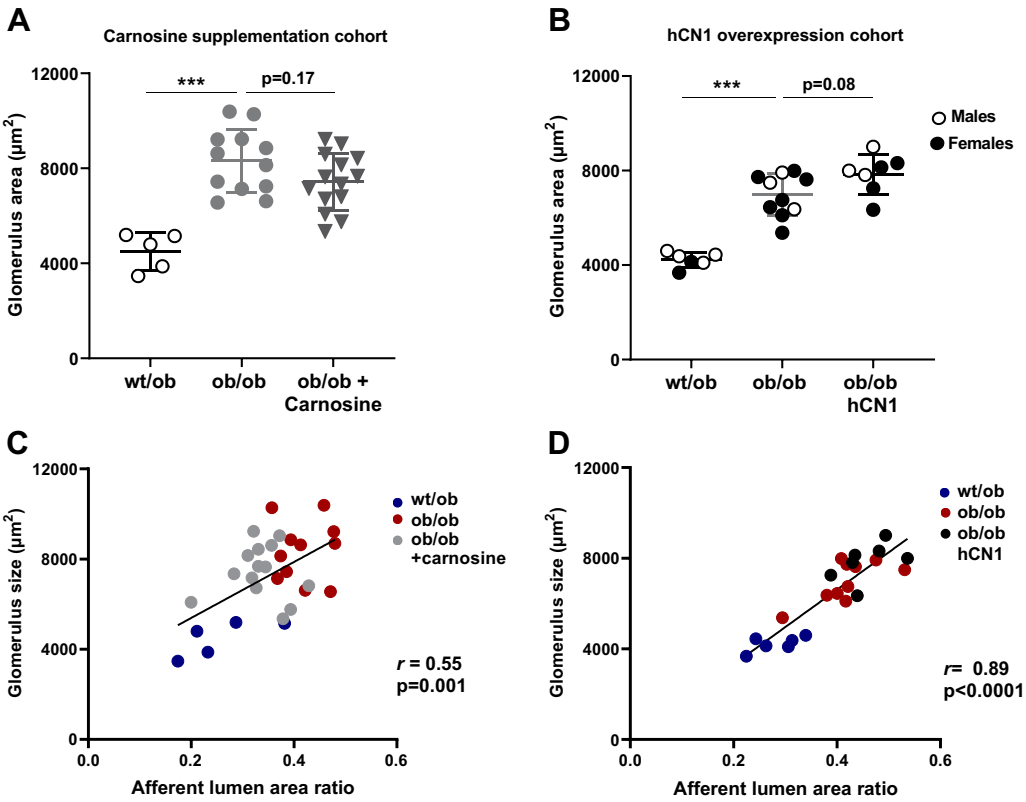

Figure 3. Effect of carnosine feeding and human carnosinase-1 (hCN1) overexpression on glomerular area. Glomerular size was significantly enlarged in two separated experimental groups of BTBR$^{ob/ob}$ mice compared with BTBR$^{wt/ob}$ mice. *A*: carnosine feeding for 18 wk in BTBR$^{ob/ob}$ mice did not significantly influence glomerulus size. *B*: in hCN1 transgenic BTBR$^{ob/ob}$ mice, glomerular area was increased compared with nontransgenic BTBR$^{ob/ob}$ mice with borderline significance. *C*: the afferent lumen (*x*-axis) was positively associated with glomerular size (*y*-axis) in BTBR$^{wt/ob}$ mice, BTBR$^{ob/ob}$ mice, and BTBR$^{ob/ob}$ mice fed with carnosine (all, $n = 30$). *D*: a similar positive correlation between afferent lumen and glomerular size was found in a separate experimental group of BTBR$^{wt/ob}$, BTBR$^{ob/ob}$, and hCN1 transgenic BTBR$^{ob/ob}$ mice (all, $n = 23$). Data are depicted as means ± SD. ***$P < 0.0001$. One-way ANOVA followed by a Tukey's post hoc test was used to compare groups.

min, $P > 0.98$). Although GFR of BTBR$^{wt/ob}$ mice displayed lower values (0.49 ± 0.13 mL/min), no significant differences were observed compared with BTBR$^{ob/ob}$ ($P = 0.32$), carnosine-supplemented ($P = 0.18$), or SGLT2-treated mice ($P = 0.39$).

DISCUSSION

In this study, we showed that carnosine supplementation presumably improves diabetes-induced intraglomerular pressure as reflected by partial normalization of the afferent arteriole lumen, whereas overexpression of CN1 had the opposite effect.

Glomerular hemodynamic dysregulation is associated with elevated intraglomerular pressure and contributes to the progression of DKD (35). In animal models, intraglomerular pressure can be measured with nephron micropuncture techniques (36), which provide a direct and true assessment of glomerular hemodynamics, yet through an invasive procedure mainly possible in species with superficial nephrons, e.g., rats and rabbits (37).

By making use of two different histological techniques, our study also showed, in independent cohorts of mice, dilation of the afferent arteriole in diabetic BTBR$^{ob/ob}$ mice relative to nondiabetic controls. This has been proposed as one of the mechanisms mediating single-nephron glomerular hyperfiltration under diabetic conditions (38). The findings from conventional histology were supported by 3D optical sectioning analysis using cleared perfused kidneys preserving vascular integrity. The molecular weight and chemical properties of the dye used herein prevented leakage to the tubuli, enabling clear visualization of branching of main vessels, afferent arterioles, and their corresponding glomerulus. This highlights the potential use of this 3D technique as an imaging tool to study pathologies where renal microvascular abnormalities are present, such as DKD.

Our study also showed that BTBR$^{ob/ob}$ mice exhibit glomerular hypertrophy, as evidenced by increased glomerular tuft area and larger Feret's diameter compared with lean healthy controls. Likewise, a positive association between Feret's diameter and afferent arteriole diameter was revealed from the 3-D analysis. These structural changes suggest that diabetic mice are hyperfiltrating and are in line with previous reports (27, 39) that showed elevated FITC-sinistrin and creatinine clearance, reflecting a state of hyperfiltration in the BTBR$^{ob/ob}$ model.

In a third cohort of wild-type, untreated diabetic, and diabetic mice treated with carnosine or an SGLT2 inhibitor (a known hyperfiltration-normalizing compound), we observed a mild tendency to hyperfiltration in the diabetic group compared with the wild-type group. Yet, GFR

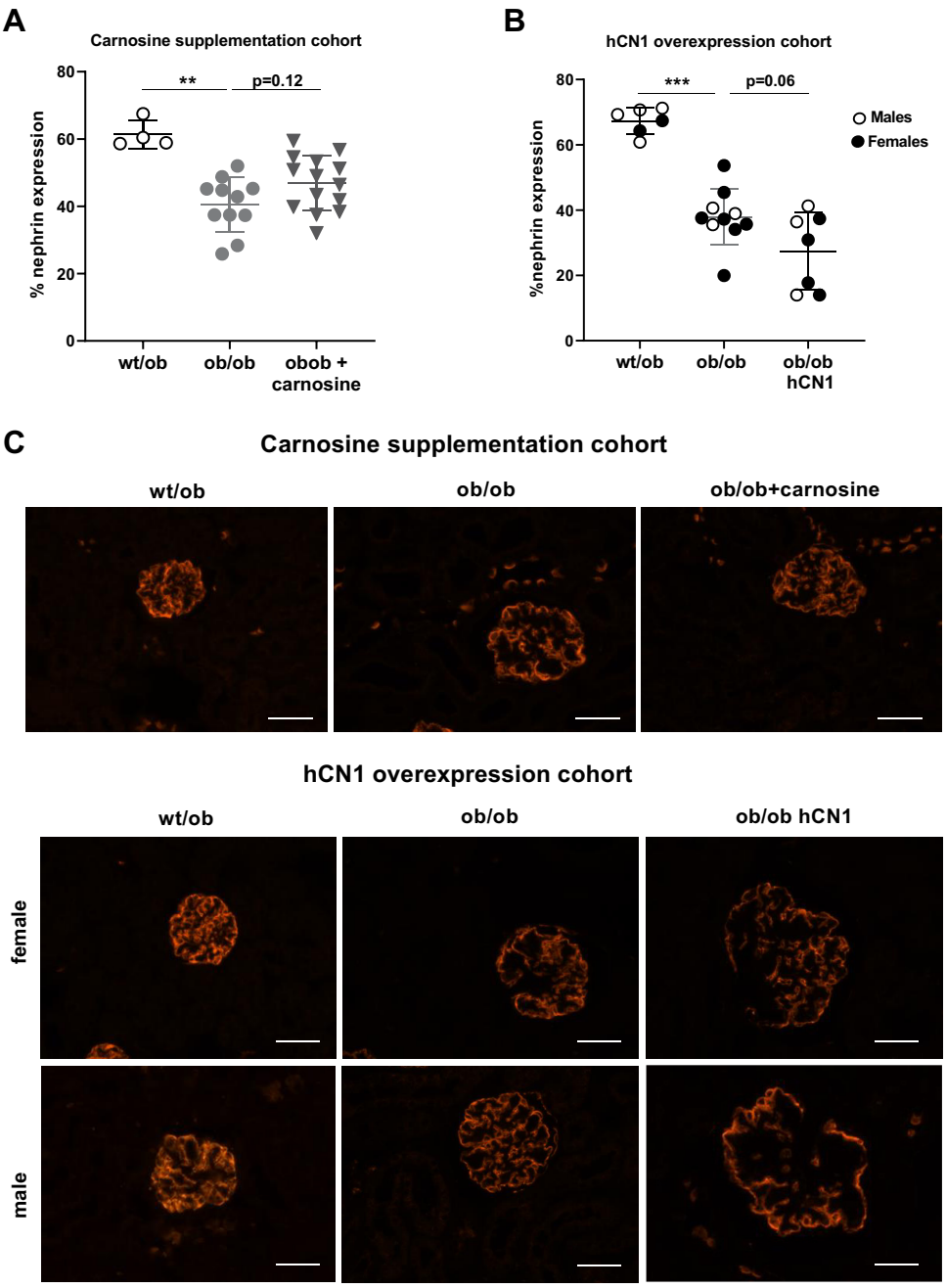

Figure 4. Effect of carnosine feeding and human carnosinase-1 (hCN1) overexpression on nephrin expression. *A*: the percentage of nephrin expression was significantly reduced in BTBR$^{ob/ob}$ mice compared with BTBR$^{wt/ob}$ mice and was not significantly affected by carnosine feeding. *B*: in a separate experimental group, the percentage of nephrin expression was further reduced in hCN1 transgenic BTBR$^{ob/ob}$ mice compared with nontransgenic BTBR$^{ob/ob}$ mice with borderline significance. *C*: representative images of glomeruli immunostained for the podocyte marker nephrin in BTBR$^{wt/ob}$ mice, BTBR$^{ob/ob}$ mice, BTBR$^{ob/ob}$ mice fed with carnosine, and hCN1 transgenic BTBR$^{ob/ob}$ mice. Scale bars = 50 μm. Data are depicted as means ± SD. $^{**}P < 0.01$ and $^{***}P < 0.0001$. One-way ANOVA followed by a Tukey's post hoc test was used to compare groups.

values did not change in the group treated with the SGLT2 inhibitor, which precludes us from drawing firm conclusions as to whether carnosine imparts an effect on diabetic-induced hyperfiltration.

Consistent with the fact that podocytes are highly sensitive to mechanical and capillary stretch (7), our study also revealed a significantly reduced expression of the podocyte slit diaphragm protein nephrin in diabetic mice. This finding is in line with the development of marked albuminuria in these animals, given the role of podocytes in maintaining the filtration barrier. Altogether, these changes are likely the reflection of an elevated intraglomerular pressure and are in accordance with studies that reported an association between diabetes and increased glomerular pressure (40, 41).

Having confirmed that in diabetic mice vasodilation of the afferent glomerular arteriole can be assessed by classical two-dimensional immune-histology, we further assessed the influence of carnosine and CN1 overexpression on afferent glomerular vasodilation using renal tissue from our previous studies. Accordingly, the major findings of our study are as follows: carnosine feeding in BTBR$^{ob/ob}$ mice reduced LAR of the afferent arteriole. In hCN1 TG BTBR$^{ob/ob}$ mice, the variation in LAR was more pronounced, possibly caused by heterogeneity in serum CN1 concentrations. This is also supported by the strong association between serum CN1 concentrations and LAR.

Glomerular hypertrophy and nephrin expression in diabetic BTBR$^{ob/ob}$ mice were neither changed by carnosine feeding nor by overexpression of hCN1, albeit that in the

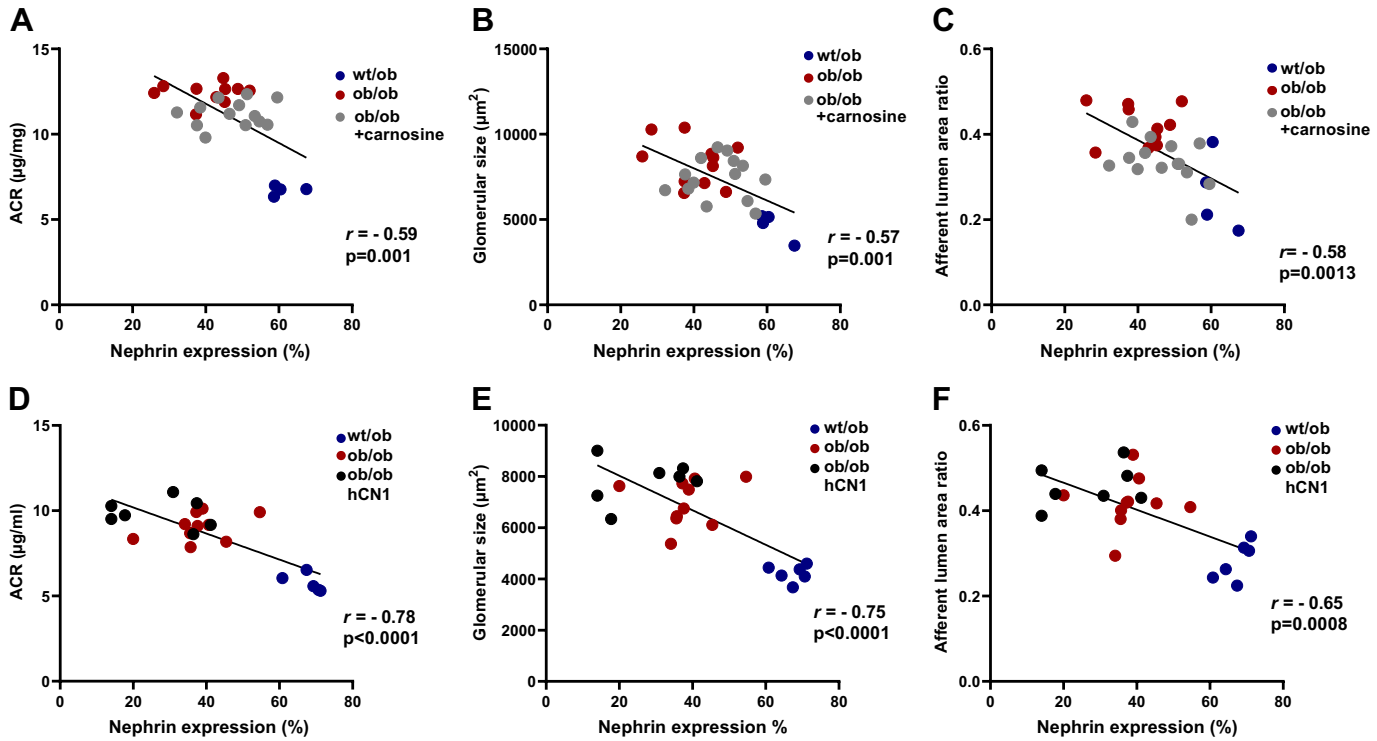

Figure 5. *A* and *D*: association between intraglomerular pressure-associated parameters. negative correlation between the percentage of nephrin expression (*x*-axis) and albuminuria [albumin-to-creatinine ratio (ACR); *y*-axis] in BTBR$^{wt/ob}$ mice, BTBR$^{ob/ob}$ mice, and BTBR$^{ob/ob}$ mice fed with carnosine (*A*) and in a separate experiment of BTBR$^{wt/ob}$, BTBR$^{ob/ob}$, and human carnosinase-1 (hCN1) transgenic BTBR$^{ob/ob}$ mice (*D*). *B* and *E*: negative association of the percentage of nephrin expression (*x*-axis) and glomerular size (*y*-axis) in BTBR$^{wt/ob}$ mice, BTBR$^{ob/ob}$ mice, and BTBR$^{ob/ob}$ mice fed with carnosine (*B*) and in a separate experiment in BTBR$^{wt/ob}$, BTBR$^{ob/ob}$, and hCN1 transgenic BTBR$^{ob/ob}$ mice (*E*). *C* and *F*: negative association between the percentage of nephrin expression (*x*-axis) and afferent lumen area (*y*-axis) in BTBR$^{wt/ob}$ mice, BTBR$^{ob/ob}$ mice, and BTBR$^{ob/ob}$ mice fed with carnosine (*C*) and in a separate experiment in BTBR$^{wt/ob}$, BTBR$^{ob/ob}$, and hCN1 transgenic BTBR$^{ob/ob}$ mice (*F*).

later mice borderline significance was observed (P = 0.08 and P = 0.06, respectively). Our study disclosed a positive association between LAR and glomerular size and a negative association between nephrin expression and albuminuria among the experimental groups. Hence, our data support the notion that carnosine/CN1 to some extent might affect intraglomerular pressure in the setting of diabetes.

However, the LAR of afferent arterioles was not different between BTBR$^{ob/ob}$ mice and hCN1 TG BTBR$^{ob/ob}$ mice. Because hCN1 TG BTBR$^{ob/ob}$ mice developed a significantly lower body weight compared with control diabetic mice, we cannot exclude this as a confounding factor. Indeed, it has been shown that obesity contributes to hyperfiltration in humans (42, 43) and in animal models (44, 45) and that body weight loss reverses hyperfiltration (46).

Moreover, as serum CN1 concentrations in hCN1 TG BTBR$^{ob/ob}$ mice strongly varied between individual mice, this also may explain why significance for LAR was not met in the comparison with wild-type BTBR$^{ob/ob}$ mice. The strong and positive association between serum CN1 concentrations and LAR of the afferent arteriole corroborates the role of CN1 on glomerular hemodynamics and, in conjunction with enhanced glomerular hypertrophy and reduced nephrin expression in hCN1 diabetic mice, explains why CN1 might have a detrimental effect on DKD development. In addition, we showed in the normalized data, significant and opposite effects on LAR of the afferent arteriole, nephrin expression, and glomerular size induced by the two interventions. In view of carnosine's beneficial properties, the marked reduction of plasma and tissue carnosine levels in hCN1 TG BTBR$^{ob/ob}$ mice might account, to some extent, for these effects. Although the intention of our study was not to assess the effect of sex on diabetes, our analyses are in line with previous reports suggesting more pronounced hyperglycemia in BTBR$^{ob/ob}$ male versus BTBR$^{ob/ob}$ female mice (24, 26). The sex-dependent effects of carnosine were not examined herein and deserve further investigation in future studies. In addition, our study suggests that sex might as well influence serum CN1 concentrations but not the lumen area of the afferent arteriole (Table 1).

In diabetes, mainly vascular and tubular mechanisms have been implicated in the pathogenesis of glomerular hyperfiltration. Yet, compelling evidence indicates that tubular events are the main trigger in this context (4). According to the tubular hypothesis, high concentrations of glucose in the diabetic filtrate enhance Na^+ reabsorption in the proximal tubule via SGLT2, resulting in increased GFR through a reduction in afferent arteriolar resistance via tubuloglomerular feedback (4).

Overexpression of CN1 did not influence the expression of proximal Na^+ transporters [SGLT1/2 or Na^+/H^+ exchanger 3 (NHE3)] in RNA-sequencing or Affymetrix analysis (data not shown). However, we cannot exclude differences in protein expression. The effect of carnosine supplementation on Na^+ transporters remains to be elucidated. Irrespective of this and given its high affinity with

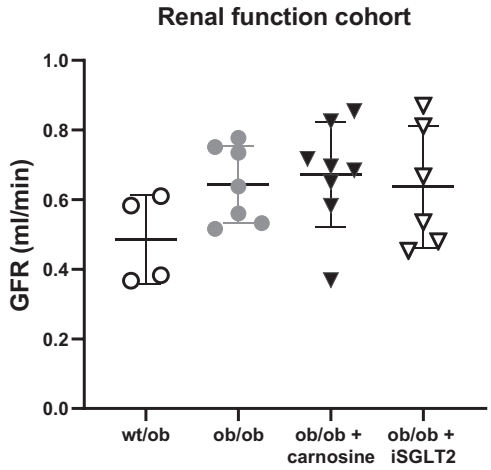

Figure 6. Effect of carnosine on glomerular filtration rate (GFR). Transcutaneous assessment of GFR using FITC-sinistrin clearance is shown. BTBR$^{ob/ob}$ mice supplemented with carnosine or treated with a hyperfiltration-normalizing compound [Na^+-glucose transporter-2 inhibitor (iSGLT2)] during 16 wk did not significantly differ from untreated diabetic mice at 24 wk of age. Age-matched wild-type mice seemingly displayed lower values of GFR. Data are depicted as means ± SD and single values. One-way ANOVA followed by a Tukey's post hoc test was used to compare groups.

protons and its buffering capacity (12), it might be that carnosine's interaction with protons impairs, to some extent, Na^+ reabsorption by NHE3 in the apical membrane of the proximal tubule. This would result in more Na^+ delivery at the macula densa, resulting in adenosine release and constriction of the afferent arteriole. Although this explanation is speculative, the work of Swietach et al. suggests, that, owing to its unique biological properties, i.e., small size (~240 Da) and titratable imidazole group (pK_a ~7), carnosine binds competitively to H^+ and acts as a diffusible cytoplasmic buffer (47, 48). Once carnosine enters epithelial cells of the proximal tubule, it is expected to achieve high cellular accumulation in this compartment (49). Although it is believed that in individuals with diabetes that proximal Na^+ reabsorption is mainly accomplished through SGLT2, accumulating evidence suggests a link between NHE3 and SGLT2 (34, 50, 51).

Insulin imbalance (deficit or hyperinsulinemia) in concert with hyperglycemia are contributing factors to the altered vascular resistance in DKD (52). As such, in hyperglycemic diabetic rats, normalization of blood glucose levels reversed intraglomerular pressure (53), and in patients with new-onset of type 2 diabetes mellitus, improvement of plasma glucose levels with initial therapy reduced GFR (54). In line with this, our study also showed a positive association between HbA1c levels and LAR.

The importance of blood glucose levels in diabetic contributors of hyperfiltration has been identified in studies showing that acute infusion of glucose increases GFR in patients with diabetes (55) and in experimental animal models (56) and inhibits the tubuloglomerular feedback response (57–59).

Carnosine supplementation has been shown to exhibit glucose-lowering effects likely through an insulinotropic action in the pancreas (13, 14, 60) and to improve insulin resistance (61). Conversely, overexpression of hCN1 resulted in worsening of the glucose profile (14, 24, 25).

Thus, if glucose concentrations are normalized early enough, it is plausible that the tubuloglomerular feedback response could be restored. Based on the available evidence, we consider that glucose-lowering effects could account for one of the primary mechanisms by which carnosine might affect the resistance of the afferent arteriole. Thus, a reduction of glucose in serum and therefore in the tubular filtrate will prevent Na^+ reabsorption by SGLT2, resulting in higher Na^+ concentrations at the macula densa, which subsequently restore the tubuloglomerular feedback response.

Although the foregoing notions in principle may explain how carnosine beneficially affects the course of DKD, further mechanistic studies are warranted to confirm or to reject these assumptions. Our work is not exempt from its own limitations, which should be considered in future studies. Possible carnosine-dependent sex differences have been disregarded, while evidence of renal transporters expression at the protein level remain to be elucidated.

Conclusions

Changes in the afferent arteriole tone can be assessed indirectly through the assessment of LAR of glomerular arterioles by conventional histopathology and optical sectioning analyses. Both imaging techniques showed dilatation of the afferent arteriole in independent sets of BTBR$^{ob/ob}$ mice as a leading event mediating increased intraglomerular pressure under diabetes conditions. Our results also provide evidence that carnosine feeding and overexpression of hCN1 likely affect intraglomerular pressure through a regulation of the afferent arteriole tone in an opposite manner. Further studies are warranted to assess the precise mechanisms by which this occurs.

SUPPLEMENTAL DATA

Supplemental Figs. S1 and S2 and Supplemental Table S1: https://doi.org/10.6084/m9.figshare.14779971.

ACKNOWLEDGMENTS

The authors thank Joana Campeiro and Wendy Dam (Department of Nephrology, UMCG) and Katharina Prem (Vth Medical Department, UMM) for the excellent technical assistance. D.O.P. thanks the data storage service SDS@hd supported by the Ministry of Science, Research and the Arts Baden-Württemberg and the German Research Foundation through Grants INST 35/1314-1 FUGG and INST 35/1503-1 FUGG and the support of the LIMa Live Cell Imaging at Microscopy Core Facility Platform Mannheim. Finally, B.A.Y. acknowledges Dr. Massimo Verzini from Flamma, Italy, for kindly providing carnosine for this project.

GRANTS

This work was supported by grants from the Deutsche Forschungsgemeinschaft (German Research Foundation) Projektnummer 392039634 and International Research Training Group 1874 DIAMICOM-SP11 (to B.A.Y.). A.R.-N. received a personal talent grant from the Graduate School of Medical Sciences of the University Medical Center Groningen, The Netherlands. D.O.P. is a recipient of a scholarship from The Ministry of Science, Research, and Arts of the State of Baden-Württemberg, Germany. S.V. has received funding from the European Union's Horizon 2020 research and innovation program under the Marie Skłodowska-Curie Grant agreement no. 813839 (RenalToolBox).

DISCLOSURES

No conflicts of interest, financial or otherwise, are declared by the authors.

AUTHOR CONTRIBUTIONS

B.A.Y. and J.v.d.B. conceived and designed research; A.R.-N., D.O.P., S.A.H., J.Q., T.A., S.V., and R.P. performed experiments; A.R.-N. and D.O.P. analyzed data; A.R.-N. and D.O.P. interpreted results of experiments; A.R.-N. and D.O.P. prepared figures; A.R.-N. drafted manuscript; A.R.-N., D.O.P., S.V., R.P., N.G., S.J.L.B., B.K.K., B.A.Y., and J.v.d.B. edited and revised manuscript; A.R.-N., D.O.P., S.A.H., J.Q., T.A., S.V., R.P., N.G., S.J.L.B., B.K.K., B.A.Y., and J.v.d.B. approved final version of manuscript.

REFERENCES

1. **Saeedi P**, **Petersohn I**, **Salpea P**, **Malanda B**, **Karuranga S**, **Unwin N**, **Colagiuri S**, **Guariguata L**, **Motala AA**, **Ogurtsova K**, **Shaw JE**, **Bright D**, **Williams R.** Global and regional diabetes prevalence estimates for 2019 and projections for 2030 and 2045: results from the International Diabetes Federation Diabetes Atlas, 9th edition. *Diabetes Res Clin Pract* 157: 107843, 2019. doi:10.1016/j.diabres.2019.107843.
2. **Tuttle KR**, **Bakris GL**, **Bilous RW**, **Chiang JL**, **De Boer IH**, **Goldstein-Fuchs J**, **Hirsch IB**, **Kalantar-Zadeh K**, **Narva AS**, **Navaneethan SD**, **Neumiller JJ**, **Patel UD**, **Ratner RE**, **Whaley-Connell AT**, **Molitch ME.** Diabetic kidney disease: a report from an ADA consensus conference. *Am J Kidney Dis* 37: 2864–2883, 2014. doi:10.1053/j.ajkd.2014.08.001.
3. **Tonneijck L**, **Muskiet MHA**, **Smits MM**, **van Bommel EJ**, **Heerspink HJL**, **van Raalte DH**, **Joles JA.** Glomerular hyperfiltration in diabetes: mechanisms, clinical significance, and treatment. *J Am Soc Nephrol* 28: 1023–1039, 2017. doi:10.1681/ASN.2016060666.
4. **Vallon V**, **Thomson SC.** The tubular hypothesis of nephron filtration and diabetic kidney disease. *Nat Rev Nephrol* 16: 317–336, 2020. doi:10.1038/s41581-020-0256-y.
5. **Sasson AN**, **Cherney DZ.** Renal hyperfiltration related to diabetes mellitus and obesity in human disease. *World J Diabetes* 3: 1–6, 2012. doi:10.4239/wjd.v3.i1.1.
6. **Jerums G**, **Premaratne E**, **Panagiotopoulos S**, **MacIsaac RJ.** The clinical significance of hyperfiltration in diabetes. *Diabetologia* 53: 2093–2104, 2010. doi:10.1007/s00125-010-1794-9.
7. **Vallon V**, **Komers R.** Pathophysiology of the diabetic kidney. *Compr Physiol* 1: 1175–1232, 2011. doi:10.1002/cphy.c100049.
8. **Magee GM**, **Bilous RW**, **Cardwell CR**, **Hunter SJ**, **Kee F**, **Fogarty DG.** Is hyperfiltration associated with the future risk of developing diabetic nephropathy? A meta-analysis. *Diabetologia* 52: 691–697, 2009. doi:10.1007/s00125-009-1268-0.
9. **Ruggenenti P**, **Porrini EL**, **Gaspari F**, **Motterlini N**, **Cannata A**, **Carrara F**, **Cella C**, **Ferrari S**, **Stucchi N**, **Parvanova A**, **Iliev I**, **Dodesini AR**, **Trevisan R**, **Bossi A**, **Zaletel J**, **Remuzzi G**, **In.** Glomerular hyperfiltration and renal disease progression in type 2 diabetes. *Diabetes Care* 35: 2061–2068, 2012. doi:10.2337/dc11-2189.
10. **Hostetter TH.** Hypertrophy and hyperfunction of the diabetic kidney. *J Clin Invest* 107: 161–162, 2001. doi:10.1172/JCI12066.
11. **Aldini G**, **de Courten B**, **Regazzoni L**, **Gilardoni E**, **Ferrario G**, **Baron G**, **Altomare A**, **D'Amato A**, **Vistoli G**, **Carini M.** Understanding the antioxidant and carbonyl sequestering activity of carnosine: direct and indirect mechanisms. *Free Radic Res* 55: 321–330, 2020. doi:10.1080/10715762.2020.1856830.
12. **Boldyrev AA**, **Aldini G**, **Derave W.** Physiology and pathophysiology of carnosine. *Physiol Rev* 93: 1803–1845, 2013. doi:10.1152/physrev.00039.2012.
13. **Albrecht T**, **Schilperoort M**, **Zhang S**, **Braun JD**, **Qiu J**, **Rodriguez A**, **Pastene DO**, **Krämer BK**, **Köppel H**, **Baelde H**, **de Heer E**, **Anna Altomare A**, **Regazzoni L**, **Denisi A**, **Aldini G**, **van den Born J**, **Yard BA**, **Hauske SJ.** Carnosine attenuates the development of both type 2 diabetes and diabetic nephropathy in BTBR$^{ob/ob}$ mice. *Sci Rep* 7: 44492, 2017. doi:10.1038/srep44492.
14. **Sauerhöfer S**, **Yuan G**, **Braun GS**, **Deinzer M**, **Neumaier M**, **Gretz N**, **Floege J**, **Kriz W**, **van der Woude F**, **Moeller MJ.** L-Carnosine, a substrate of carnosinase-1, influences glucose metabolism. *Diabetes* 56: 2425–2432, 2007. doi:10.2337/db07-0177.
15. **Aldini G**, **Orioli M**, **Rossoni G**, **Savi F**, **Braidotti P**, **Vistoli G**, **Yeum KJ**, **Negrisoli G**, **Carini M.** The carbonyl scavenger carnosine ameliorates dyslipidaemia and renal function in Zucker obese rats. *J Cell Mol Med* 15: 1339–1354, 2011. doi:10.1111/j.1582-4934.2010.01101.x.
16. **Soliman KM**, **Mohamed AM**, **Metwally NS.** Attenuation of some metabolic deteriorations induced by diabetes mellitus using carnosine. *J Appl Sci* 7: 2252–2260, 2007. doi:10.3923/jas.2007.2252.2260.
17. **Riedl E**, **Pfister F**, **Braunagel M**, **Brinkkötter P**, **Sternik P**, **Deinzer M**, **Bakker SJL**, **Henning RH**, **van den Born J**, **Krämer BK**, **Navis G**, **Hammes H-P**, **Yard B**, **Koeppel H.** Carnosine prevents apoptosis of glomerular cells and podocyte loss in STZ diabetic rats. *Cell Physiol Biochem* 28: 279–288, 2011. doi:10.1159/000331740.
18. **Ahluwalia TS**, **Lindholm E**, **Groop LC.** Common variants in CNDP1 and CNDP2, and risk of nephropathy in type 2 diabetes. *Diabetologia* 54: 2295–2302, 2011. doi:10.1007/s00125-011-2178-5.
19. **Freedman BI**, **Hicks PJ**, **Sale MM**, **Pierson ED**, **Langefeld CD**, **Rich SS**, **Xu J**, **McDonough C**, **Janssen B**, **Yard BA**, **van der Woude FJ**, **Bowden DW.** A leucine repeat in the carnosinase gene CNDP1 is associated with diabetic end-stage renal disease in European Americans. *Nephrol Dial Transplant* 22: 1131–1135, 2007. doi:10.1093/ndt/gfl717.
20. **Janssen B**, **Hohenadel D**, **Brinkkoetter P**, **Peters V**, **Rind N**, **Fischer C**, **Rychlik I**, **Cerna M**, **Romzova M**, **de Heer E**, **Baelde H**, **Bakker SJL**, **Zirie M**, **Rondeau E**, **Mathieson P**, **Saleem MA**, **Meyer J**, **KöPpel H**, **Sauerhoefer S**, **Bartram CR**, **Nawroth P**, **Hammes H-P**, **Yard BA**, **Zschocke J**, **van der Woude FJ.** Carnosine as a protective factor in diabetic nephropathy: association with a leucine repeat of the carnosinase gene CNDP1. *Diabetes* 54: 2320–2327, 2005. doi:10.2337/diabetes.54.8.2320.
21. **Mooyaart AL**, **van Valkengoed IGM**, **Shaw PKC**, **Peters V**, **Baelde HJ**, **Rabelink TJ**, **Bruijn JA**, **Stronks K**, **de Heer E.** Lower frequency of the 5/5 homozygous CNDP1 genotype in South Asian Surinamese. *Diab Res Clin Pract* 85: 272–278, 2009. doi:10.1016/j.diabres.2009.06.001.
22. **Mooyaart AL**, **Zutinic A**, **Bakker SJL**, **Grootendorst DC**, **Kleefstra N**, **van Valkengoed IGM**, **Bohringer S**, **Bilo HJG**, **Dekker FW**, **Bruijn JA**, **Navis G**, **Janssen B**, **Baelde HJ**, **De Heer E.** Association between CNDP1 genotype and diabetic nephropathy is sex specific. *Diabetes* 59: 1555–1559, 2010. doi:10.2337/db09-1377.
23. **Riedl E**, **Koeppel H**, **Brinkkoetter P**, **Sternik P**, **Steinbeisser H**, **Sauerhoefer S**, **Janssen B**, **van der Woude FJ**, **Yard BA.** A CTG polymorphism in the CNDP1 gene determines the secretion of serum carnosinase in Cos-7 transfected cells. *Diabetes* 56: 2410–2413, 2007. doi:10.2337/db07-0128.
24. **Everaert I**, **He J**, **Hanssens M**, **Stautemas J**, **Bakker K**, **Albrecht T**, **Zhang S**, **Van der Stede T**, **Vanhove K**, **Hoetker D**, **Howsam M**, **Tessier FJ**, **Yard B**, **Baba SP**, **Baelde HJ**, **Derave W.** Carnosinase-1 overexpression, but not aerobic exercise training, affects the development of diabetic nephropathy in BTBR$^{ob/ob}$ mice. *Am J Physiol Renal Physiol* 318: F1030–F1040, 2020. doi:10.1152/ajprenal.00329.2019.
25. **Qiu J**, **Albrecht T**, **Zhang S**, **Hauske SJ**, **Rodriguez-Niño A**, **Zhang X**, **Nosan D**, **Pastene DO**, **Sticht C**, **Delatorre C**, **van Goor H**, **Porubsky S**, **Krämer BK**, **Yard BA.** Human carnosinase 1 overexpression aggravates diabetes and renal impairment in BTBR$^{ob/ob}$ mice. *J Mol Med* 98: 1333–1346, 2020. doi:10.1007/s00109-020-01957-0.
26. **Hudkins KL**, **Pichaiwong W**, **Wietecha T**, **Kowalewska J**, **Banas MC**, **Spencer MW**, **Mühlfeld A**, **Koelling M**, **Pippin JW**, **Shankland SJ**, **Askari B**, **Rabaglia ME**, **Keller MP**, **Attie AD**, **Alpers CE.** BTBR$^{ob/ob}$ mutant mice model progressive diabetic nephropathy. *J Am Soc Nephrol* 21: 1533–1542, 2010. doi:10.1681/ASN.2009121290.
27. **Ericsson A**, **Tonelius P**, **Lal M**, **Sabirsh A**, **Böttcher G**, **William-Olsson L**, **Strömstedt M**, **Johansson C**, **Hyberg G**, **Tapani S**, **Jönsson-Rylander AC**, **Unwin R.** The effects of dual PPARα/γ agonism compared with ACE inhibition in the BTBRob/ob mouse model of diabetes and diabetic nephropathy. *Physiol Rep* 5: e13186, 2017. doi:10.14814/phy2.13186.
28. **Schreiber A**, **Shulhevich Y**, **Geraci S**, **Hesser J**, **Stsepankou D**, **Neudecker S**, **Koenig S**, **Heinrich R**, **Hoecklin F**, **Pill J**, **Friedemann J**, **Schweda F**, **Gretz N**, **Schock-Kusch D.** Transcutaneous measurement of renal function in conscious mice. *Am J Physiol Renal Physiol* 303: F783–F788, 2012. doi:10.1152/ajprenal.00279.2012.
29. **Adelmann K**, **Frey D**, **Riedl E**, **Koeppel H**, **Pfister F**, **Peters V**, **Schmitt CP**, **Sternik P**, **Hofmann S**, **Zentgraf HW**, **Navis G**, **van den Born J**, **Bakker SJL**, **Krämer BK**, **Yard BA**, **Hauske SJ.** Different

conformational forms of serum carnosinase detected by a newly developed sandwich ELISA for the measurements of carnosinase concentrations. *Amino Acids* 43: 143–151, 2012. doi:10.1007/s00726-012-1244-8.

30. **Huang J**, **Brenna C**, **Khan A. U M**, **Daniele C**, **Rudolf R**, **Heuveline V**, **Gretz N.** A cationic near infrared fluorescent agent and ethyl-cinnamate tissue clearing protocol for vascular staining and imaging. *Sci Rep* 9: 521, 2019. doi:10.1038/s41598-018-36741-1.
31. **Bolte S**, **Cordelières FP.** A guided tour into subcellular colocalization analysis in light microscopy. *J Microsc* 224: 213–232, 2006. doi:10.1111/j.1365-2818.2006.01706.x.
32. **Ollion J**, **Cochennec J**, **Loll F**, **Escudé C**, **Boudier T.** TANGO: a generic tool for high-throughput 3D image analysis for studying nuclear organization. *Bioinformatics* 29: 1840–1841, 2013. doi:10.1093/bioinformatics/btt276.
33. **Krebs C**, **Hamming I**, **Sadaghiani S**, **Steinmetz OM**, **Meyer-Schwesinger C**, **Fehr S**, **Stahl RAK**, **Garrelds IM**, **Danser AHJ**, **Van Goor H**, **Contrepas A**, **Nguyen G**, **Wenzel U.** Antihypertensive therapy upregulates renin and (pro)renin receptor in the clipped kidney of Goldblatt hypertensive rats. *Kidney Int* 72: 725–730, 2007. doi:10.1038/sj.ki.5002408.
34. **Uijl E**, **'T Hart DC**, **Roksnoer LCW**, **Groningen M. C C-V**, **van Veghel R**, **Garrelds IM**, **de Vries R**, **van der Vlag J**, **Zietse R**, **Nijenhuis T**, **Joles JA**, **Hoorn EJ**, **Danser AHJ.** Angiotensin-neprilysin inhibition confers renoprotection in rats with diabetes and hypertension by limiting podocyte injury. *J Hyperten* 38: 755–764, 2020. doi:10.1097/HJH.0000000000002326.
35. **Helal I**, **Fick-Brosnahan GM**, **Reed-Gitomer B**, **Schrier RW.** Glomerular hyperfiltration: definitions, mechanisms and clinical implications. *Nat Rev Nephrol* 8: 293–300, 2012. doi:10.1038/nrneph.2012.19.
36. **Vallon V.** Micropuncturing the nephron. *Pflugers Arch* 458: 189–201, 2009. doi:10.1007/s00424-008-0581-7.
37. **Denton KM**, **Anderson WP.** Glomerular ultrafiltration in rabbits with superficial glomeruli. *Pflugers Arch* 419: 235–242, 1991. doi:10.1007/BF00371101.
38. **Brenner BM**, **Lawler EV**, **Mackenzie HS.** The hyperfiltration theory: a paradigm shift in nephrology. *Kidney Int* 49: 1774–1777, 1996. doi:10.1038/ki.1996.265.
39. **Gembardt F**, **Bartaun C**, **Jarzebska N**, **Mayoux E**, **Todorov VT**, **Hohenstein B**, **Hugo C.** The SGLT2 inhibitor empagliflozin ameliorates early features of diabetic nephropathy in BTBR *ob/ob* type 2 diabetic mice with and without hypertension. *Am J Physiol Renal Physiol* 307: F317–F325, 2014. doi:10.1152/ajprenal.00145.2014.
40. **Bjornstad P**, **Sõkrtić M**, **Lytvyn Y**, **Maahs DM**, **Johnson RJ**, **Cherney DZI.** The Gomez equations and renal hemodynamic function in kidney disease research. *Am J Physiol Renal Physiol* 311: F967–F975, 2016. doi:10.1152/ajprenal.00415.2016.
41. **Hashimoto S**, **Yamada K**, **Kawata T**, **Mochizuki T**, **Schnermann J**, **Koike T.** Abnormal autoregulation and tubuloglomerular feedback in prediabetic and diabetic OLETF rats. *Am J Physiol Renal Physiol* 296: F598–F604, 2009. doi:10.1152/ajprenal.00074.2008.
42. **Chagnac A**, **Herman M**, **Zingerman B**, **Erman A**, **Rozen-Zvi B**, **Hirsh J**, **Gafter U.** Obesity-induced glomerular hyperfiltration: its involvement in the pathogenesis of tubular sodium reabsorption. *Nephrol Dial Transplant* 23: 3946–3952, 2008. doi:10.1093/ndt/gfn379.
43. **Chagnac A**, **Weinstein T**, **Korzets A**, **Ramadan E**, **Hirsch J**, **Gafter U.** Glomerular hemodynamics in severe obesity. *Am J Physiol Renal Physiol* 278: F817–F822, 2000. doi:10.1152/ajprenal.2000.278.5.F817.
44. **Bivona BJ**, **Park S**, **Harrison-Bernard LM.** Glomerular filtration rate determinations in conscious type II diabetic mice. *Am J Physiol Renal Physiol*, 300: F618–F625, 2011. doi:10.1152/ajprenal.00421.2010.
45. **Henegar JR**, **Bigler SA**, **Henegar LK**, **Tyagi SC**, **Hall JE.** Functional and structural changes in the kidney in the early stages of obesity. *J Am Soc Nephrol* 12: 1211–1217, 2001. doi:10.1681/ASN.V1261211.
46. **Chagnac A**, **Weinstein T**, **Herman M**, **Hirsh J**, **Gafter U**, **Ori Y.** The effects of weight loss on renal function in patients with severe obesity. *J Am Soc Nephrol* 14: 1480–1486, 2003. doi:10.1097/01.ASN.0000068462.38661.89.
47. **Swietach P**, **Leem CH**, **Spitzer KW**, **Vaughan-Jones RD.** Pumping Ca^{2+} up H^+ gradients: a Ca^{2+}-H^+ exchanger without a membrane. *J Physiol* 592: 3179–3188, 2014. doi:10.1113/jphysiol.2013.265959.
48. **Swietach P**, **Youm JB**, **Saegusa N**, **Leem CH**, **Spitzer KW**, **Vaughan-Jones RD.** Coupled Ca^{2+}/H^+ transport by cytoplasmic buffers regulates local Ca^{2+} and H^+ ion signaling. *Proc Natl Acad Sci USA* 110: E2064–E2073, 2013. doi:10.1073/pnas.1222433110.
49. **Jappar D**, **Hu Y**, **Keep RF**, **Smith DE.** Transport mechanisms of carnosine in SKPT cells: contribution of apical and basolateral membrane transporters. *Pharm Res* 26: 172–181, 2009. doi:10.1007/s11095-008-9726-9.
50. **Beloto-Silva O**, **Machado UF**, **Oliveira-Souza M.** Glucose-induced regulation of NHEs activity and SGLTs expression involves the PKA signaling pathway. *J Membrane Biol* 239: 157–165, 2011. doi:10.1007/s00232-010-9334-6.
51. **Onishi A**, **Fu Y**, **Patel R**, **Darshi M**, **Crespo-Masip M**, **Huang W**, **Song P**, **Freeman B**, **Kim YC**, **Soleimani M**, **Sharma K**, **Thomson SC**, **Vallon V.** A role for tubular Na^+/H^+ exchanger NHE3 in the natriuretic effect of the SGLT2 inhibitor empagliflozin. *Am J Physiol Renal Physiol* 319: F712–F728, 2020. doi:10.1152/ajprenal.00264.2020.
52. **Arima S**, **Ito S.** The mechanisms underlying altered vascular resistance of glomerular afferent and efferent arterioles in diabetic nephropathy. *Nephrol Dial Transplant* 18: 1966–1969, 2003. doi:10.1093/ndt/gfg263.
53. **Stackhouse S**, **Miller PL**, **Park SK**, **Meyer TW.** Reversal of glomerular hyperfiltration and renal hypertrophy by blood glucose normalization in diabetic rats. *Diabetes* 39: 989–995, 1990. doi:10.2337/diabetes.39.8.989.
54. **Vora JP**, **Dolben J**, **Williams JD**, **Peters JR**, **Owens DR.** Impact of initial treatment on renal function in newly-diagnosed type 2 (non-insulin-dependent) diabetes mellitus. *Diabetologia* 36: 734–740, 1993. doi:10.1007/BF00401144.
55. **Christiansen JS**, **Frandsen M**, **Parving HH.** Effect of intravenous glucose infusion on renal function in normal man and in insulin-dependent diabetics. *Diabetologia* 21: 368–373, 1981. doi:10.1007/BF00252683.
56. **Noonan WT**, **Shapiro VM**, **Banks RO.** Renal glucose reabsorption during hypertonic glucose infusion in female streptozotocin-induced diabetic rats. *Life Sci* 68: 2967–2977, 2001. doi:10.1016/S0024-3205(01)01090-6.
57. **Levine DZ**, **Iacovitti M**, **Robertson SJ.** Modulation of single-nephron GFR in the db/db mouse model of type 2 diabetes mellitus. II. Effects of renal mass reduction. *Am J Physiol Regul Integr Comp Physiol* 294: R1840–R1846, 2008. doi:10.1152/ajpregu.00457.2007.
58. **Levine DZ**, **Iacovitti M**, **Robertson SJ**, **Mokhtar GA.** Modulation of single-nephron GFR in the db/db mouse model of type 2 diabetes mellitus. *Am J Physiol Regul Integr Comp Physiol* 290: R975–R981, 2006. doi:10.1152/ajpregu.00693.2005.
59. **Thomson SC**, **Deng A**, **Bao D**, **Satriano J**, **Blantz RC**, **Vallon V.** Ornithine decarboxylase, kidney size, and the tubular hypothesis of glomerular hyperfiltration in experimental diabetes. *J Clin Invest* 107: 217–224, 2001. doi:10.1172/JCI10963.
60. **Cripps MJ**, **Hanna K**, **Lavilla C**, **Sayers SR**, **Caton PW**, **Sims C**, **De Girolamo L**, **Sale C**, **Turner MD.** Carnosine scavenging of glucolipotoxic free radicals enhances insulin secretion and glucose uptake. *Sci Rep* , 7: 13313, 2017. doi:10.1038/s41598-017-13649-w.
61. **de Courten B**, **Jakubova M**, **de Courten MP**, **Kukurova IJ**, **Vallova S**, **Krumpolec P**, **Valkovic L**, **Kurdiova T**, **Garzon D**, **Barbaresi S**, **Teede HJ**, **Derave W**, **Krssak M**, **Aldini G**, **Ukropec J**, **Ukropcova B.** Effects of carnosine supplementation on glucose metabolism: Pilot clinical trial. *Obesity (Silver Spring)* 24: 1027–1034, 2016. doi:10.1002/oby.21434.